MCB
Journals.ASM.org

In Vivo Interaction Proteomics Reveal a Novel p38 Mitogen-Activated Protein Kinase/Rack1 Pathway Regulating Proteostasis in *Drosophila* Muscle

Vladimir E. Belozerov,[a] Srdjana Ratkovic,[b,c] Helen McNeill,[b,c] Arthur J. Hilliker,[a] John C. McDermott[a]

Department of Biology, York University, Toronto, Canada[a]; Samuel Lunenfeld Research Institute, Mount Sinai Hospital, Toronto, Canada[b]; Department of Molecular Genetics, University of Toronto, Toronto, Canada[c]

Several recent studies suggest that systemic aging in metazoans is differentially affected by functional decline in specific tissues, such as skeletal muscle. In *Drosophila*, longevity appears to be tightly linked to myoproteostasis, and the formation of misfolded protein aggregates is a hallmark of senescence in aging muscle. Similarly, defective myoproteostasis is described as an important contributor to the pathology of several age-related degenerative muscle diseases in humans, e.g., inclusion body myositis. p38 mitogen-activated protein kinase (MAPK) plays a central role in a conserved signaling pathway activated by a variety of stressful stimuli. Aging p38 MAPK mutant flies display accelerated motor function decline, concomitant with an enhanced accumulation of detergent-insoluble protein aggregates in thoracic muscles. Chemical genetic experiments suggest that p38-mediated regulation of myoproteostasis is not limited to the control of reactive oxygen species production or the protein degradation pathways but also involves upstream turnover pathways, e.g., translation. Using affinity purification and mass spectrometry, we identified Rack1 as a novel substrate of p38 MAPK in aging muscle and showed that the genetic interaction between *p38b* and *Rack1* controls muscle aggregate formation, locomotor function, and longevity. Biochemical analyses of Rack1 in aging and stressed muscle suggest a model whereby p38 MAPK signaling causes a redistribution of Rack1 between a ribosome-bound pool and a putative translational repressor complex.

Physiologic analyses of aging in humans (1) and recent molecular genetic studies in model metazoans raise a compelling possibility that the systemic functional decline characteristic of aging is a consequence of local degenerative changes in specific tissues (2). Not surprisingly, skeletal muscle, with its large metabolic and endocrine potential, emerged as an important regulator of systemic longevity. For example, modulating the activity of the TOR pathway in the muscle tissue in *Drosophila* (3) and *Caenorhabditis elegans* causes significant changes in longevity. However, the molecular signals that trigger muscle aging in a normal physiological context are more complex and not completely understood.

A central role in the aging of postmitotic cells is attributed to the system of mechanisms that control the concentration, conformation, and location of cellular proteins, known as proteostasis (4). Proteostatic dysfunction in neurons is a well-established cause of common neurodegenerative syndromes, such as Parkinson's and Alzheimer's diseases (5). In skeletal muscle dysregulated proteostasis manifests in a similar pathology (6). Insoluble protein aggregates accumulate in the sarcoplasm, myonuclei, and endomysium, in time causing myofiber degeneration. This results in a wide spectrum of pathologies collectively known as protein aggregate myopathies (PAMs). Genetic forms of PAM are linked to mutations in a diverse group of muscle proteins with both structural (e.g., myosin, desmin, plectin, and titin) and nonstructural (e.g., DNAJB6, BAG-3, and PABPN1) functions (7). However, the most common PAM in the elderly, known as sporadic inclusion body myositis (sIBM), has not been linked to any specific single-gene alleles (8, 9). Importantly, both hereditary PAM and sporadic IBM patients display wide heterogeneity in the onset time and severity of pathological symptoms. This clinical observation raises the possibility that genetic variations in myoproteostatic pathways among patients are sufficiently potent to modify the pathogenic activity of aggregation-prone proteins. Little is currently known of the PAM-modifying cellular mechanisms, and no effective therapeutic treatments are available for these progressive debilitating diseases. The use of genetically tractable model systems to study proteostasis (10), especially in the context of PAM, holds great promise for eventual therapeutic intervention. Since adult *Drosophila* muscles recapitulate many of the molecular, structural, and functional elements of the skeletal muscle tissue in vertebrates (11), the fly emerged as a useful model for study of myoproteostasis.

Three fly models of PAM have been constructed. Muscle pathology in these models was achieved by tissue-specific expression of human proteins (APP [12], PABPN1 [13], and E706K mutant myosin heavy chain IIa [14]) known to cause aggregate formation. All of these models recapitulate key features of human disease, namely, age-dependent aggregate formation, locomotor function loss, and reduced life-span. Experimental manipulation of proteostasis modifies these phenotypes. For example, coexpression of an E3 ubiquitin ligase Parkin largely rescues the effects of APP, and overexpression of the Hsp70 pathway components or viral anti-

Received 26 June 2013 Returned for modification 22 July 2013
Accepted 12 November 2013
Published ahead of print 25 November 2013
Address correspondence to John C. McDermott, jmcderm@yorku.ca.
Supplemental material for this article may be found at http://dx.doi.org/10.1128/MCB.00824-13.

doi:10.1128/MCB.00824-13

apoptotic protein p35 attenuates the PABPN1 phenotype. Two other pathways with prominent roles in proteostasis in aging *Drosophila* muscle were recently examined. The first study found that manipulation of FOXO activity is linked to age-related deposition of polyubiquitylated aggregates in thoracic muscle. FOXO acts through its transcription target 4E-BP/Thor to potentiate autophagy thereby enhancing the turnover of damaged proteins (3). FOXO and Thor are downstream components of the insulin/IGF signaling pathway that is recognized as a key regulator of functional senescence and longevity in a variety of models. However, contributions from other signaling pathways are also being examined. One example is the p38 mitogen-activated protein kinase (MAPK) pathway. Although the role of p38 in mammalian myogenesis is well established (reviewed in references 15 and 16), less is known about its function in aging muscle. A recent study demonstrated that p38b, one of two p38 MAPKs in *Drosophila*, modulates reactive oxygen species (ROS)-mediated damage in thoracic muscle (17). At least two pathways appear to be involved: Mef2-driven expression of MnSOD (Sod2) and Nrf2-dependent suppression of Keap1. Thus, p38b-deficient animals show elevated levels of oxidatively damaged proteins in muscle and a reduced life-span.

We report here that p38b deficiency leads to the accelerated deposition of polyubiquitylated protein aggregates in thoracic muscles of aging flies, a cellular pathology likely connected to previously reported locomotor phenotypes and reduced longevity in these animals. By using a chemical genetic approach, we show that the effects of p38b on myoproteostasis are not limited to ROS-dependent mechanisms but also involve regulation of protein synthesis. Finally, we present the results of an *in vivo* proteomic screen for muscle-specific substrates of p38b and identify and characterize Rack1 as a novel substrate that may directly control the rate of protein translation in response to p38b signaling.

MATERIALS AND METHODS

Fly genetics and drug treatments. Flies were raised on a standard cornmeal-agar-molasses medium at 25°C. *p38bΔ45* and upstream activation sequence (UAS)-*p38bKD* flies were previously described (17). UAS-*Sod2* and *GMR-Gal4* flies were kindly donated by A. Hilliker and H. McNeill, respectively. UAS-*p38b IR*, UAS-*Rack1 IR*, *Mef2-Gal4*, $Rack1^{1.8}$, $Rack1^{EE}$, and $Rack1^{EY128}$ flies were obtained from the Bloomington *Drosophila* Stock Center. For drug treatments, flies were starved for 6 h and transferred onto 5% sucrose–1% low-melting temperature agarose (Gibco) medium supplemented with 5 mM paraquat (Sigma), 600 μM puromycin (Sigma), 20 mM chloroquine (BioShop), 50 μM MG132 (Sigma), and 10 μM chelerythrine chloride (BioShop).

Climbing assay and longevity scoring. Climbing ability was measured in a simple negative geotaxis assay by counting the number of flies that reach the top of the vial (top 20% of the length) in 5 s after tapping and dividing by the total number of flies. Twenty flies were tested per genotype-treatment combination, and measurements were repeated three times. For life-span measurements, flies were kept on standard food at 20 flies per vial and transferred to fresh vials every 3 days. Surviving flies were counted every 24 h.

Western blot and dot blot analyses of thoracic muscle extracts. To isolate detergent-soluble and insoluble protein extracts, we modified a method described previously (18). Fifteen thoraces for each age and genotype were freshly prepared and homogenized in 300 μl of buffer A (20 mM Tris-HCl [pH 8.0], 150 mM NaCl, 1 mM EDTA, 1% Triton X-100, 0.1% sodium dodecyl sulfate [SDS], 0.5% sodium deoxycholate, 0.5% protease inhibitor cocktail [Sigma], 5 mM NaF, 10 mM sodium β-glycerophosphate, 1 mM Na_3VO_4). Lysates were incubated on ice for 30 min with occasional vortexing and centrifuged at 16,000 × *g* for 15 min at 4°C. Supernatants represented the detergent-soluble protein fraction. Pellets were resuspended in 100 μl of buffer B (10 mM Tris-HCl [pH 7.5], 1% SDS, 0.5% protease inhibitor cocktail [Sigma], 5 mM NaF, 10 mM sodium β-glycerophosphate, 1 mM Na_3VO_4), sonicated for 1 min (6 × 10 s pulses), and incubated at room temperature for 30 min. Extracts were cleared by centrifugation at 500 × *g* for 10 min at room temperature, yielding detergent-insoluble fractions. The total protein concentration in extracted fractions was determined by using the Dc protein assay (Bio-Rad), and normalized samples were run on SDS–10% PAGE gels, followed by standard Western blotting procedure. For dot blot analyses 3-μl samples were applied onto nitrocellulose membrane (Bio-Rad) and allowed to dry overnight. Membranes were subsequently hydrated and washed in Tris-buffered saline for 30 min at room temperature, followed by incubation with the Odyssey blocking solution (LI-COR), respective primary antibodies, and near-infrared fluorophore-labeled secondary antibodies (goat anti-rabbit antibody 680RD and goat anti-mouse antibody 800CW; LI-COR). Imaging and quantification were performed using the Odyssey system (LI-COR), and aggregate levels were calculated as ratios of the ubiquitin and histone H3 fluorescent signals normalized by values in wild-type flies.

The following antibodies were used throughout the study: antiubiquitin (mouse monoclonal, P4D1; Cell Signaling), antiactin (rabbit polyclonal, I-19-R; Santa Cruz Biotechnology), anti-histone H3 (rabbit monoclonal; Cell Signaling), anti-Rack1 (rabbit monoclonal, D59D5; Cell Signaling), anti-S6 (mouse monoclonal, 54D2; Cell Signaling), anti-phospho-p38 MAPK (rabbit polyclonal, Thr180 Tyr182; Cell Signaling), anti-*Drosophila* p38 (goat polyclonal, dN-20; Santa Cruz Biotechnology), anti-FLAG (mouse monoclonal, M2; Sigma), anti-phospho-ATF2 (rabbit polyclonal, Thr71; Cell Signaling), and antipuromycin (mouse monoclonal, 3RH11; KeraFast).

Immunoprecipitations and liquid chromatography-tandem mass spectrometry (LC-MS/MS) proteomics. The expression levels of the p38bKD bait were examined in all pairwise combinations of three muscle-specific drivers (MHC-Gal4, Mef2-Gal4, and 1151-Gal4) and two independent UAS-p38bKD responder lines. Most of these combinations produced significantly higher levels of p38bKD compared to endogenous p38 (data not shown). For proteomic analysis, we chose the Mef2-Gal4 driver that produced a <2-fold higher level of p38bKD compared to the endogenous level (see Fig. 4A).

Transgenic flies expressing FLAG-tagged p38bKD and control w^{1118} flies were aged at 25°C, anesthetized, and dissected. Individual thoraces were immediately frozen on dry ice. Fifty thoraces were used in a typical immunoprecipitation, and 100 thoraces per biological replicate were used in proteomic analyses. Thorax samples were thawed on ice and homogenized in lysis buffer described previously (19) with 10 to 15 strokes of a Dounce homogenizer on ice. Lysates were frozen on dry ice, thawed, and centrifuged at 14,000 × *g* for 15 min. Cleared lysates were incubated with anti-FLAG M2 magnetic beads (Sigma) for 2 h at 4°C. Immunoprecipitations of S2 cell lysates were performed as described earlier (19). After the incubations, the beads were washed, and bound proteins were digested with trypsin and identified using a Thermo LTQ XL mass spectrometer coupled to a nano-LC system (Agilent). The results of Mascot searches were sorted using ProHits software (20). Final data set consisted of four biological replicates for p38KD bait and w^{1118} control samples (see Data Set S1 in the supplemental material). Proteins identified in both the bait and the control samples were considered nonspecific and removed from subsequent analyses, with the exception of glycogen synthase that was >10-fold more abundant in bait samples compared to controls. We also removed proteins that were identified in fewer than two biological replicates and proteins identified by a single peptide or short peptides (i.e., <10 amino acids in length).

Recombinant Rack1 and kinase assays. Full-length human RACK1 cDNA (MGC) was expressed as an N-terminal MBP fusion (pMAL system; New England BioLabs) in BL21(DE3) *Escherichia coli* grown at 37°C

and induced with 0.5 mM IPTG (isopropyl-β-D-thiogalactopyranoside) for 2 h. Bacteria were lysed by sonication on ice, and soluble MBP-RACK1 was purified using amylose resin (New England BioLabs) according to the manufacturer's protocol and buffer exchanged into 25 mM Tris (pH 7.5)–25 mM NaCl. FLAG-tagged p38 kinase constructs were transfected into S2 cells, and cells were stimulated with 10 mM H_2O_2 for 45 min. Active p38 kinases were purified using anti-FLAG magnetic beads (Sigma) as described previously (19). Kinase reactions were assembled by mixing purified MBP-RACK1 with bead-bound kinases in 25 mM Tris (pH 7.5), 5 mM β-glycerophosphate, 2 mM dithiothreitol (DTT), 0.1 mM Na_3VO_4, 10 mM $MgCl_2$, and 200 μM ATP. After a 30-min incubation at 30°C, the magnetic beads were removed, and phosphorylated substrate was repurified using an amylose affinity matrix. Phosphorylation was detected by Western blotting with anti-phospho-Ser and anti-phospho-Thr antibodies (Millipore).

***In vitro* translation assays.** Protocols for extract preparation and translation reactions were adapted from earlier studies (21, 22). Briefly, thoraces were lysed in 10 mM HEPES (pH 7.4), 5 mM DTT, and 1× complete protease inhibitor cocktail (Roche) and cleared by centrifugation at 14,000 × *g* at 4°C for 15 min. Micrococcal nuclease (New England BioLabs) at 0.15 U/μl and 1 mM $CaCl_2$ were added, and the extract was incubated for 4 min at 20°C, followed by the addition of 2 mM EGTA. Translation reaction mixtures included 40% extract, 50 mM CH_3COOK, 0.5 mM $(CH_3COO)_2Mg$, 60 μM amino acid mix (Promega), 0.1 mM spermidine, 20 U of RNase inhibitor (Fisher) per reaction, 0.1 μg of creatine kinase (Sigma)/μl, 20 mM creatine phosphate (BioShop), and 0.03 pmol of firefly luciferase mRNA (Promega) per reaction. Luciferase light units were normalized by the protein concentration in thoracic extracts.

Ribosomal fractionation. Thoraces dissected from aged or puromycin-fed flies were homogenized in 20 mM Tris (pH 7.4), 140 mM KCl, 5 mM $MgCl_2$, 0.5 mM DTT, 1% Triton X-100, 0.1 mg of cycloheximide (Sigma)/ml, 1 mg of heparin/ml, and 50 U of RNase inhibitor (Fisher)/ml and cleared by centrifugation at 14,000 × *g* for 10 min at 4°C (23). Supernatants were then fractionated by using a 10 to 50% discontinuous sucrose gradient centrifugation at 35,000 rpm for 2 h at 4°C. Twelve fractions were collected after centrifugation and used for Western blot analyses and semiquantitative reverse transcription-PCR (RT-PCR).

RESULTS

Dysregulation of protein homeostasis in thoracic muscles of p38b mutant flies. Since previous work described age-related motor deficits in p38b-null flies (17), we tested whether an abnormal accumulation of misfolded protein in thoracic muscles may be associated with the observed functional decline. Ample evidence suggests that the aggregation state of intracellular misfolded proteins determines their cytotoxic effect. Therefore, we adapted a two-step protein extraction procedure in which a soluble fraction is isolated in a mild Triton X-100-containing buffer and the remaining aggregate fraction is solubilized in the presence of 1% SDS. Samples derived from the thoraces of age-matched wild-type and p38b mutant flies were examined by Western blotting with an antiubiquitin antibody (Fig. 1A). To more accurately quantify the levels of ubiquitin conjugates in thorax extracts, we used dot blotting and near-infrared fluorescence intensity measurement (Fig. 1B to D). Higher levels of protein ubiquitylation are seen in soluble and aggregate fractions from p38b mutant flies compared to wild-type controls irrespective of age (Fig. 1A). Importantly, the accumulation of ubiquitin conjugates in the aggregate fractions from mutant flies becomes more pronounced in 30-day-old flies (Fig. 1C), a finding consistent with the age-related decline in motor function.

ROS-independent control of myoproteostasis by p38b. Control of the oxidative damage caused by ROS in the adult fly muscle has emerged as a key mechanism linking p38b activity to life-span (17). In the proposed pathway, p38b potentiates the Mef2-driven expression of the mitochondrial superoxide dismutase (Sod2), thereby limiting the effects of ROS (Fig. 2F). Consistent with this model, transgenic overexpression of Sod2 in muscle tissue rescues the effect of p38b deficiency on longevity (17). Therefore, we sought to explore the link between the enhanced protein aggregation we observed in p38b mutant muscle and ROS induction.

First, we compared the levels of ubiquitylated aggregates in the thoraces of 1-week-old flies reared on normal food. As expected, aggregates were elevated in flies with a muscle-specific (Mef2-Gal4 driver, Fig. 2A) knockdown of p38b compared to the wild-type control (Fig. 2E). However, the introduction of ectopic Sod2 (Fig. 2B) into the p38b-knockdown animals caused only a minor reduction in aggregate formation (Fig. 1E). Next, we tested whether aggregate formation can be enhanced by a potent systemic ROS induction and the ability of p38b and Sod2 to mediate this process. By using a GSTD1-green fluorescent protein (GFP) transgene as a sensor of oxidative stress, we determined that a 16-h exposure of

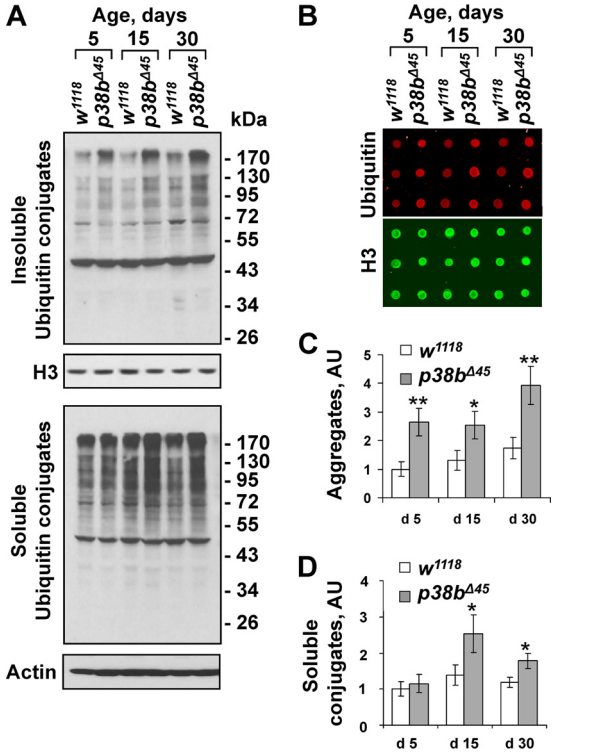

FIG 1 p38MAPK regulates protein aggregate accumulation in aging thoracic muscle. (A) Enhanced accumulation of ubiquitylated protein aggregates in thoracic muscles of p38b-deficient flies. Triton X-100-insoluble (top) and Triton X-100-soluble (bottom) protein extracts were prepared from the thoraces of wild-type (w^{1118}) and isogenic *p38b*-null ($p38b^{\Delta 45}$) flies at 5, 15, and 30 days after eclosion. The levels of ubiquitylated conjugates were assayed using an antiubiquitin antibody. Actin and histone H3 were used as loading controls for soluble and insoluble extracts, respectively. (B) The levels of ubiquitylated aggregates were quantified by dot blot analyses using near-infrared fluorescent detection (see Materials and Methods). Dot blot assays were performed in triplicates. Red fluorescent signal (ubiquitin) was divided by green signal (histone H3) and normalized by the w^{1118} control at day 5. A representative dot blot with aggregate samples is shown. (C and D) Quantification of ubiquitin conjugates in aggregate and detergent-soluble fractions. Columns represent means ± the standard errors (SD; $n = 3$; NS, not significant; *, $P < 0.05$ [unpaired two-tailed Student *t* test]).

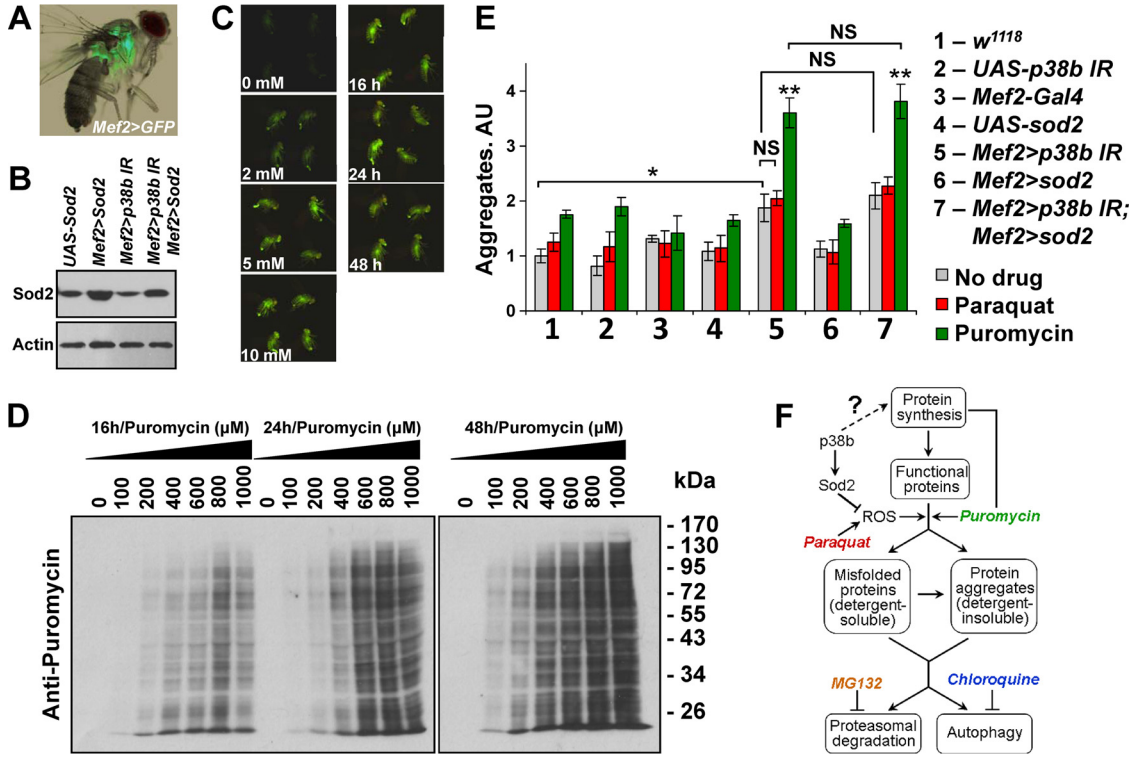

FIG 2 p38MAPK regulates protein aggregate accumulation independently of ROS control. (A) *Mef2-Gal4* driver used throughout the study directs tissue-specific expression in adult thoracic muscle (visualized by UAS-*GFP*). (B) Ectopic expression of MnSOD (Sod2) in thoracic muscle. Thoracic extracts from flies carrying indicated transgenes were examined by Western blotting. *Mef2-Gal4* driver was used to express UAS-*Sod2* and UAS-*p38b IR* responders. (C) Flies carrying a glutathione *S*-transferase D1 (GSTD1)–GFP construct were fed paraquat-supplemented food (concentrations are indicated below the images), and GFP expression was documented at 24 h (left row). Images for four flies from replicate vials are shown as fluorescent photographs. No increase in GFP intensity is observed at between 5 and 10 mM paraquat. GSTD1-GFP flies were fed 5 mM paraquat-supplemented food and imaged at the indicated time points. Robust activity of the GSTD1 promoter is observed at 16 h after treatment (right row). (D) Incorporation of puromycin into polypeptides in thoracic muscle was examined by feeding w^{1118} flies drug-supplemented food, followed by Western blotting. The following concentrations of puromycin were tested at each of the indicated time points: 0, 100, 200, 400, 600, 800, and 1,000 μM. Puromycin effectively incorporates into newly synthesized peptides at 16 h and a concentration greater than 400 μM. (E) p38b may control aggregate deposition independently of the Mef2/Sod2 pathway. The effect of a 16-h exposure to oxidative (paraquat) and proteotoxic (puromycin) stress on protein aggregate deposition in muscle was measured by dot blot analyses of extracts. Inverted-repeat-based RNAi line (UAS-*p38b IR*) was used to knock down p38b expression. The effects of drug treatments were confirmed by using a GSTD1-GFP reporter and Western blotting for paraquat and puromycin, respectively. Columns represent means ± the SD ($n = 3$; NS, not significant; *, $P < 0.05$; **, $P < 0.01$ [unpaired two-tailed Student *t* test]). (F) Schematic representation of main proteostatic pathways. Chemical modulators of proteostasis are color-coded to match the bar graphs in panel and Fig. 3B.

flies to 5 mM paraquat is sufficient to induce ROS systemically (Fig. 2C). These conditions were then used to examine the effect of ROS induction on aggregate deposition. One-week-old flies were fed 5 mM paraquat for 16 h, followed by protein extraction and dot blot analysis of ubiquitylated aggregates. A small increase (<25%) in aggregate levels was observed in wild-type and p38b-knockdown flies, compared to respective levels in flies fed unsupplemented food. A similar increase was also seen in p38b-knockdown flies overexpressing Sod2 (Fig. 2E). These observations suggest that p38b deficiency does not significantly enhance aggregate deposition in response to transient ROS induction and that the ROS-neutralizing activity of Sod2 is insufficient to suppress aggregate formation caused by p38b deficiency.

Finally, we examined the role of p38b and Sod2 in a ROS-independent model of aggregate induction. Puromycin is an aminoacyl tRNA analog that binds to the ribosome and blocks polypeptide chain elongation, causing the premature release of truncated proteins. When the synthesis of these truncations overwhelms protein clearance pathways, they may contribute to aggregate formation. We monitored the incorporation of puromycin moieties into polypeptide chains by Western blotting (Fig. 2D) and then fed 1-week-old flies with 600 μM puromycin-supplemented food for 16 h prior to aggregate extraction. Indeed, an ~80% increase in aggregate level was recorded in wild-type and p38b mutant flies compared to controls fed unsupplemented food (Fig. 2E). Importantly, the levels of aggregates in p38-deficient animals were unaffected by the ectopic expression of Sod2. Collectively, these data suggest that ROS-mediated damage is insufficient to account for the effect of p38b deficiency on protein aggregate deposition.

p38b may be involved in controlling protein synthesis in thoracic muscle. Since Sod2 does not fully rescue the effects of p38b deficiency on aggregate formation in muscle, we conclude that there is an additional ROS-independent mechanism(s) of p38b-mediated control of myoproteostasis. Translation is a central node of protein turnover known to receive inputs from a variety of signaling pathways, most prominently TOR. To test the possibility that p38b signaling also contributes to translational control in

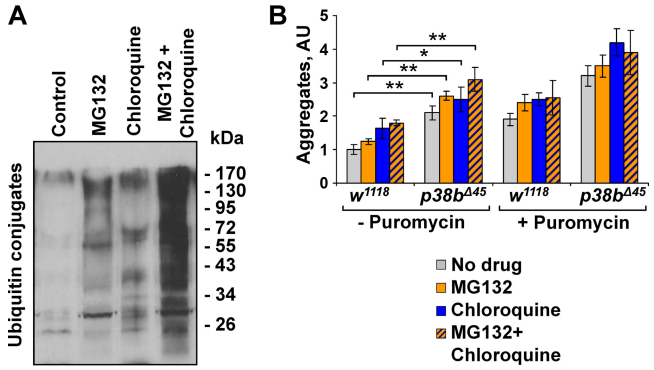

FIG 3 p38b controls myoproteostasis upstream of protein degradation pathways. (A) Feeding w^{1118} flies food supplemented with 50 μM MG132, 20 mM chloroquine, and a combination of the two drugs leads to a robust accumulation of ubiquitylated proteins in thoracic muscle compared to untreated controls. Western blots of thoracic muscle extracts are shown. (B) Proteasome activity and autophagy were inhibited by treating *w1118* and $p38b^{\Delta 45}$ with MG132 and chloroquine, respectively. Additional proteotoxic stress was induced by puromycin. Aggregate levels in thoraces were determined by dot blot. Columns represent means ± the SD ($n = 3$; NS, not significant; *, $P < 0.05$; **, $P < 0.01$ [unpaired two-tailed Student *t* test]).

muscle, we first sought to determine whether p38b controls aggregate formation upstream of the degradation pathways (Fig. 2F). We utilized an *in vivo* chemical genetic approach. One-week-old wild-type and p38b mutant flies were fed potent inhibitors of proteasome (MG132) and autophagy (chloroquine) in the absence (Fig. 3A) or in the presence of puromycin. After drug treatment, the levels of detergent-insoluble ubiquitin conjugates in fly thoraces were determined by dot blot analysis (Fig. 3B). Both inhibitors caused moderate increase in insoluble aggregates in wild-type muscle, and demonstrated additivity. We reasoned that if p38b acted solely at the level of protein degradation, treatment with MG132 and chloroquine would be expected to counteract the effect of p38b deficiency. In contrast to this prediction, we observed significantly higher levels of muscle aggregates in inhibitor-fed p38-mutant flies compared to wild-type controls. These differences were even more pronounced when inhibitor treatments were performed in the presence of puromycin (Fig. 3B). Collectively, these results suggest that p38b signaling affects myoproteostasis upstream of the degradation pathways, which is consistent with a possible role for p38b in protein synthesis.

***In vivo* proteomic screen for muscle-specific p38b substrates.** There are only a few characterized substrates of the *Drosophila* p38 kinases, and no substrates directly involved in translational regulation have been previously reported (19). To examine muscle-specific substrate repertoire of p38b *in vivo*, we utilized a substrate trap approach (24, 25). A FLAG-tagged kinase-dead mutant of p38b (p38bKD) was expressed in thoracic muscles (Fig. 4A), affinity purified, and analyzed by mass spectrometry to identify copurifying proteins. Some of the proteins in the isolated complexes are expected to represent bona fide substrates trapped

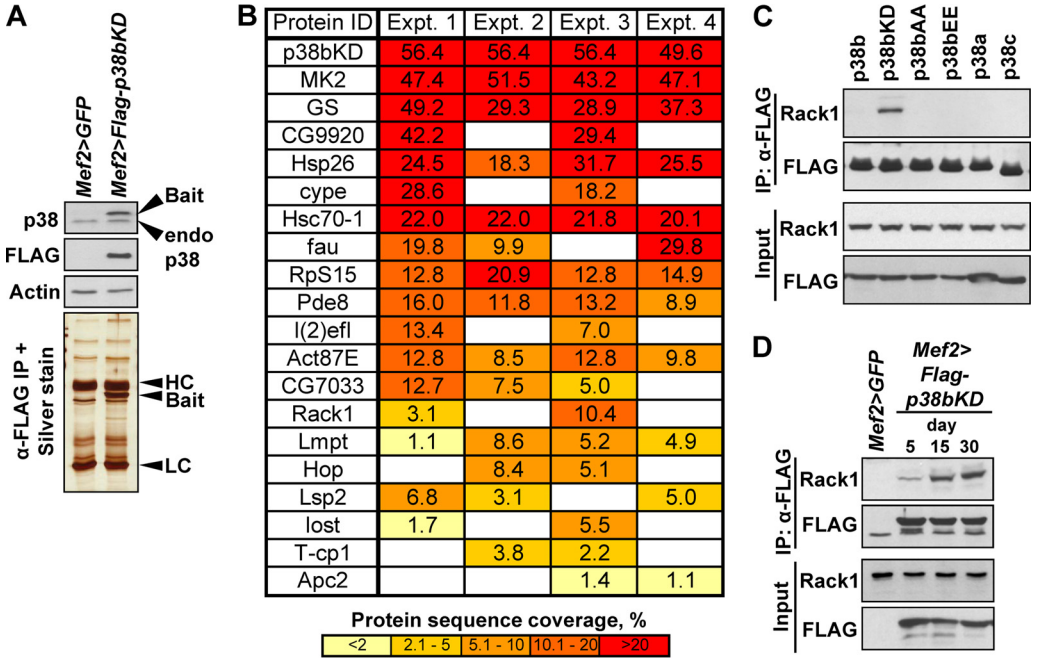

FIG 4 Interaction proteomics identify Rack1 as a binding partner of p38bKD in adult thoracic muscle. (A) The *Mef2>p38bKD* transgenic flies express FLAG-p38bKD (bait) at a level comparable to endogenous p38b (Western blot, top). p38bKD and associated proteins are recovered from thorax extracts using a one-step affinity purification (silver stained gel, bottom) and subjected to LC-MS/MS analysis. HC, IgG heavy chain; LC, IgG light chain. (B) List of p38bKD interacting proteins identified by proteomics (see Materials and Methods for details). The results from four independent biological replicate (experiments 1 to 4) analyses are shown. The percent protein sequence coverage is shown for each interacting protein, with respective color coding shown below the table. (C) The interaction of Rack1 and p38b was confirmed by coimmunoprecipitation of endogenous Rack1 in S2 cells transiently transfected with FLAG-tagged wild-type p38 kinases, and three p38b mutants, p38bAA (T183A/Y185A), p38bEE (T183E/Y185E), and p38bKD (K53R). No interaction is observed between Rack1 and related kinases, p38a and p38c. Among the p38b constructs only the kinase-dead mutant shows robust interaction, a finding consistent with the substrate-trap model. (D) The p38bKD-Rack1 interaction is enhanced in aging flies. Coimmunoprecipitations were performed using thoraces of 5-, 15-, and 30-day-old *Mef2>p38bKD* flies, and the levels of endogenous Rack1 in precipitates were determined by Western blotting.

in unproductive interactions with the catalytically inactive kinase. We performed four replicate purifications of p38bKD complexes from 15-day-old flies in parallel with the four control purifications (see Materials and Methods). Only the interacting proteins specific to p38bKD samples and found in two or more replicates were considered. Since a large number of factors contribute to the stoichiometry of the inactive kinase-substrate binding, no ranking of potential substrates based on protein coverage was performed. A total of 19 putative substrates (Fig. 4B) were identified, including previously characterized substrates MK2 and glycogen synthase. One of the isolated proteins, receptor of activated C kinase 1 (Rack1) is a component of the 40S ribosomal subunit known to regulate translation initiation (26). We hypothesized that Rack1 may serve as a link between p38b signaling and translational regulation and thus chose this interactor for further analysis despite its relatively low protein coverage.

p38b binds to and phosphorylates Rack1 *in vitro*. To verify the interaction of p38b and Rack1, we expressed FLAG-tagged versions of wild-type p38b, p38bKD, as well as related kinases p38a and p38c in *Drosophila* S2 cells, and tested whether endogenous Rack1 can be detected in kinase immunoprecipitates. As shown in Fig. 4C, Rack1 specifically binds to p38bKD but not the wild-type p38b or two activation loop mutants, a finding consistent with the model of substrate trapping. No binding is observed between Rack1 and p38a or p38c. Similarly, p38bKD binds to the endogenous Rack1 *in vivo*, and the interaction appears stronger in older flies (Fig. 4D). In S2 cells p38b forms stable complexes with MK2 and other partners (19), raising the possibility that Rack1 associates with p38b through other complex components. Therefore, we performed *in vitro* binding assays using bacterially expressed p38b and Rack1 and confirmed direct physical interaction between the two proteins (Fig. 5A). Next, we sought to determine whether Rack1 can serve as a substrate for activated p38b. S2 cells were transfected with wild-type p38b, p38bKD, and p38a, and respective kinases were immunoprecipitated from unstimulated cells or cells exposed to oxidative stress (H_2O_2). Bacterially expressed MBP-Rack1 fusion was incubated with p38 kinases bound to beads, and at the end of reaction Rack1 was repurified using amylose-agarose and tested for the presence of phosphorylation by Western blotting with anti-phospho-Ser and anti-phospho-Thr antibodies. To confirm the kinase activity of p38 in these assays, we set up a parallel set of reactions with a known p38 substrate ATF2 (Fig. 5B). Stress-activated p38b but not p38a was able to phosphorylate both Ser and Thr residues in Rack1. These phosphorylation events are attributed to the kinase activity of p38b, since no phospho-signal was detected in p38bKD reactions, and the level of phosphorylation was significantly reduced in the presence of SB203580, a specific p38 inhibitor.

The interaction with Rack1 does not modulate p38b activity. Several binding partners of p38 kinases have been shown to affect the kinase activity by serving as scaffolds for the upstream kinases, chaperones for nucleocytoplasmic shuttling, and other mechanisms (27). Therefore, we tested whether the interaction with Rack1 may modulate some aspect of p38b activity *in vivo*. One-week-old flies with muscle-specific knockdown of Rack1 (*Mef2>Rack1 IR*) and driver-only controls were exposed to a 37°C heat shock to activate p38, and thorax lysates were analyzed by Western blotting (Fig. 5C). Despite a noticeable depletion of Rack1 in the *Mef2>Rack1 IR* animals, no significant changes were observed in the levels of total p38 or stress-induced phospho-p38.

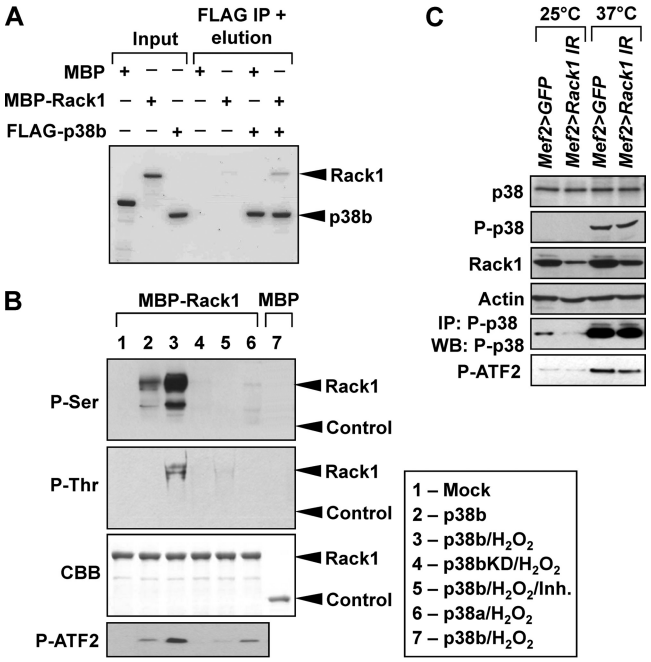

FIG 5 Rack1 acts as a direct substrate of p38b without affecting its kinase activity. (A) Bacterially expressed MBP-Rack1 and FLAG-p38b exhibit binding in a pulldown assay, confirming their direct interaction. Proteins were visualized by Coomassie blue staining. Bands corresponding to p38b and Rack1 are marked. Band densitometry showed that ca. 5% of input Rack1 bound to p38b, a finding consistent with a transient kinase-substrate interaction. (B) S2 cells were transfected with the indicated FLAG-tagged p38MAPK constructs and stimulated by 10 mM H_2O_2 for 30 min. Kinases were then purified from S2 lysates by FLAG-immunoprecipitation and used in *in vitro* kinase assays with MBP-Rack1. MBP and ATF2 were used as controls. Inh, 10 μM SB203580. Following the kinase reactions, MBR-Rack1 was repurified by using amylose beads, and its phosphorylation was determined by Western blotting. The location of bands corresponding to MBP-Rack1 (Rack1) and MBP (Control) are indicated. The composition of the *in vitro* kinase reactions corresponding to gel lanes is shown in the box. (C) The p38b level and activity were examined in the muscle of unstressed (25°C) or heat-shocked (37°C, 30 min) Rack1 knockdown (*Mef2>Rack1 IR*) and control (*Mef2>GFP*) flies. Levels of total and phospho-p38b (T183, Y185) were determined by Western blotting and show no change in response to Rack1 depletion. Activated endogenous P-p38 was immunoprecipitated from thorax extracts and assayed *in vitro* using a recombinant substrate ATF2. The kinase activity of P-p38 appears unchanged in *Mef2>Rack1 IR* flies compared to controls.

Next, doubly phosphorylated p38 was immunoprecipitated from thorax lysates and used in *in vitro* kinase assays with recombinant ATF2 (Fig. 5C). Approximately equal levels of phospho-ATF2 were detected in these reactions, indicating that the level of Rack1 in thoracic muscles does not influence catalytic activity of p38b.

Genetic interaction between p38b and Rack1 enhances accumulation of protein aggregates in muscle and controls life-span and locomotor function. Based on our biochemical results, we reasoned that p38b and Rack1 may share a genetic pathway. We first tested this possibility in the eye. Homozygous p38b mutant flies ($p38b^{\Delta 45}$) exhibit a slight rough-eye phenotype compared to wild-type w^{1118} eyes (Fig. 6A, top row). In contrast, no ommatidial defects are observed in p38b heterozygotes ($p38b^{\Delta 45/+}$), and minimal ommatidial pattern disruption is seen in the flies with an eye-specific knockdown of Rack1 (*GMR>Rack1 IR*). However, Rack1 depletion combined with one copy of the p38b-null allele ($p38b^{\Delta 45/+}$ *GMR>Rack1 IR*) produces rough eyes that are re-

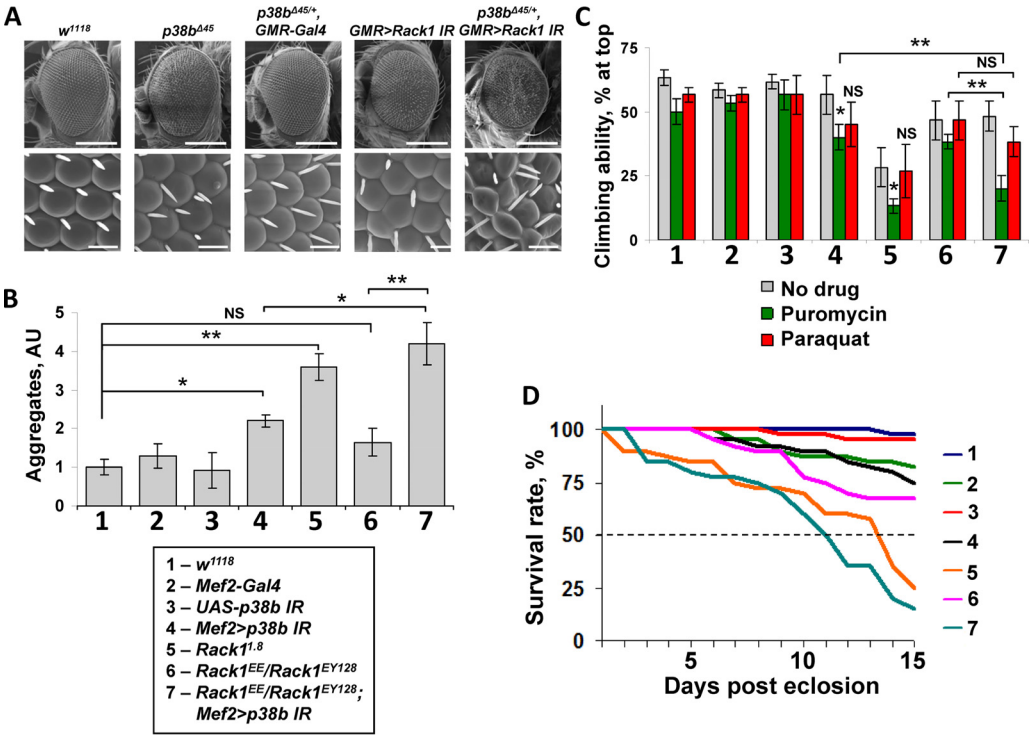

FIG 6 Rack1 and p38b genetically interact to control myoproteostasis, locomotor function, and life-span. (A) Eye phenotypes of animals carrying *p38b* and *Rack1* alleles were documented by scanning electron microscopy. Top row, ×150 magnification, 200-μm scale bar. Bottom row, ×2,000 magnification, 15-μm scale bar. Smaller rough eyes are observed when an eye-specific knockdown of Rack1 (*GMR>Rack1 IR*) is combined with a heterozygous *p38b*-null allele (*p38bΔ45*). (B) Thoracic aggregate deposition is largely unaffected in a *Rack1* hypomorphic background ($Rack1^{EE}/Rack1^{EY128}$) compared to wild-type control. However, aggregate formation is strongly potentiated by combining these *Rack1* alleles with a *p38b* knockdown (*Mef2>p38b IR*). Aggregate levels were measured by dot blot in thoracic extracts from 3-day-old flies (see Materials and Methods). (C) Three-day-old flies were fed paraquat or puromycin, and subjected to a simple negative geotaxis assay. Genetic interaction of $Rack1^{EE}/Rack1^{EY128}$ and *Mef2>p38b IR* greatly reduces locomotor function under proteotoxic stress. In panels B and C, columns represent means ± the SD ($n = 3$; NS, not significant; *, $P < 0.05$; **, $P < 0.01$ [unpaired two-tailed Student *t* test]). (D) Life-span was evaluated in flies of indicated genotypes by scoring survival under normal conditions (25°C, unsupplemented food) over a period of 15 days. Dashed line indicates median survival. A markedly decreased life-span is observed in $Rack1^{EE}/Rack1^{EY128}$; *Mef2>p38b IR* flies.

duced in size (Fig. 6A), indicating dominant interaction of the two alleles and suggesting that p38b and Rack1 likely function in the same pathway.

We next tested whether the observed genetic interaction affects the deposition of insoluble aggregates in thoracic muscle. For these tests, we used flies carrying a homozygous Rack1-null allele ($Rack1^{1.8}$) that express no detectable Rack1 protein and a transheterozygous combination of strong hypomorphic alleles ($Rack1^{EE}/Rack1^{EY128}$) that express greatly reduced levels of Rack1 (28). Interestingly, thoracic muscles of the Rack1-null animals contain high levels of insoluble aggregates, whereas the levels found in the hypomorphs are not significantly higher than those in wild-type flies (Fig. 6B). However, when p38b is depleted by RNA interference (RNAi; *Mef2>p38b IR*) in the $Rack1^{EE}/Rack1^{EY128}$ background the levels of muscle aggregates are dramatically elevated and exceed those observed in the *Mef2>p38b IR* thoraces in the presence of wild-type levels of Rack1 (Fig. 6B).

We reasoned that the insoluble aggregates accumulating in the muscles of the Rack1 and p38b mutants may impact locomotor function and longevity in these animals. To test these possibilities we performed negative geotaxis assays using 3-day-old animals of indicated genotypes (Fig. 6C) reared on normal food. At this age, only the homozygous $Rack1^{1.8}$ flies showed significantly reduced climbing ability. Therefore, we subjected these animals to additional proteotoxic and oxidative stresses by providing them with puromycin and paraquat supplemented food for 24 h. Under these conditions puromycin-fed flies demonstrated the most pronounced changes. The climbing ability of the Rack1-null flies deteriorated further and, importantly, the $Rack1^{EE}/Rack1^{EY128}$; *Mef2>p38b IR* flies suffered a >2-fold decline in locomotor function compared to the drug-free control. In contrast, paraquat feeding produced only minor changes in climbing ability that were restricted to animals with the reduced levels of p38b, independently of the Rack1 background. These data indicate that the p38b-Rack1 interaction modulates locomotor function in response to proteotoxic but not oxidative stress.

Finally, we sought to correlate the above molecular and functional observations with the longevity of flies with respective allelic combinations (Fig. 6D). Indeed, the $Rack1^{1.8}$ homozygotes and the $Rack1^{EE}/Rack1^{EY128}$; *Mef2>p38b IR* flies demonstrated the shortest life-span, a finding consistent with the levels of aggregate accumulation in thoracic muscles, and sensitivity to proteotoxic stress.

p38b/Rack1 pathway affects translation rate in muscle. Given the sensitivity of p38b and Rack1 double-mutant flies to proteotoxic stress and the involvement of Rack1 in translational regulation, we hypothesized that Rack1 may serve as a link between p38b signaling and protein synthesis control. To test this,

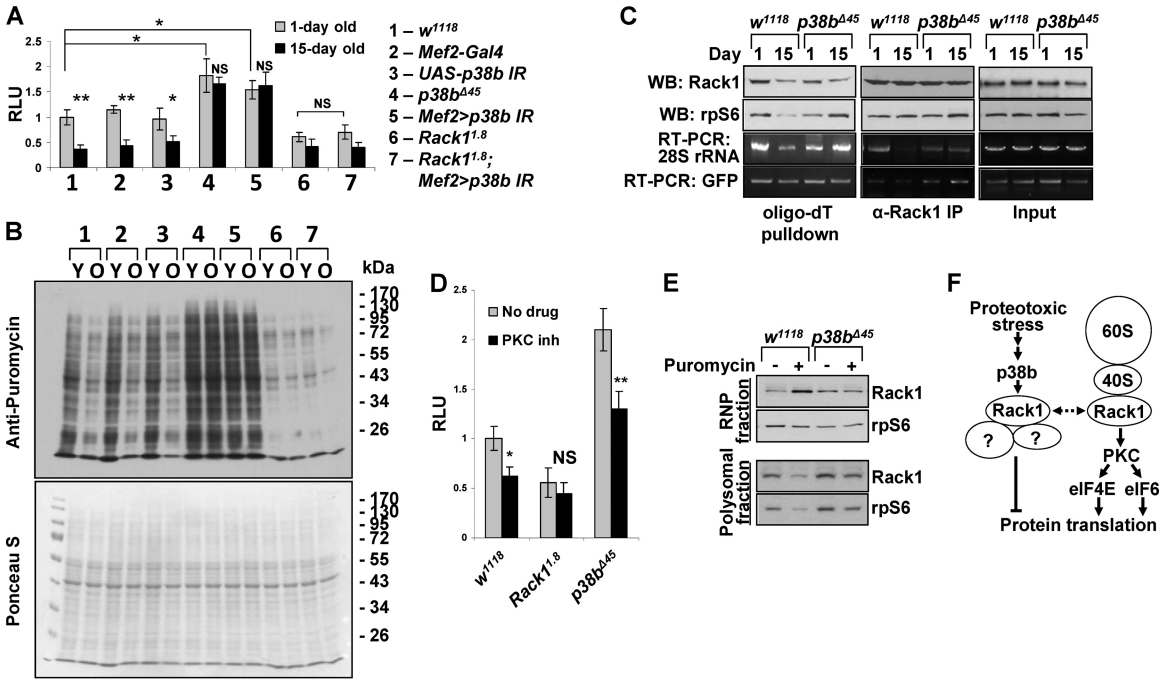

FIG 7 p38b-Rack1 pathway controls translation rates in aging muscle. (A) *In vitro* translation assays were performed with thoracic extracts from 1- and 15-day-old flies using a synthetic firefly luciferase mRNA reporter (see Materials and Methods). Columns represent means ± the SD ($n = 3$; NS, not significant; *, $P < 0.05$; **, $P < 0.01$ [unpaired two-tailed Student *t* test]). (B) Translation rates were measured *in vivo* by feeding flies of the indicated genotypes (same as in panel A) 600 μM puromycin for 24 h. After treatment, thoracic extracts were analyzed by Western blotting with an antipuromycin antibody. Total protein was visualized by Ponceau-S staining. Y, young, 1-day-old flies; O, old, 15-day-old flies. (C) Changes in the association of Rack1 and ribosomal subunits with mRNA in aging wild-type and *p38b*-deficient flies were examined by oligo(dT) pulldown and anti-Rack1 immunoprecipitation. rpS6 and 28S rRNA were used as representative components of 40S and 60S ribosomal subunits. RNA levels were determined by semiquantitative RT-PCR. (D) The p38b-Rack1 and Rack1-PKC pathways appear to operate in parallel to affect translation rate in *Drosophila* muscle. Wild-type (w^{1118}) and Rack1 ($Rack1^{1.8}$)- and p38b ($p38b^{\Delta 45}$)-null mutants were fed chelerythrin chloride-supplemented food (PKC inh), followed by the measurement of translational activity in thoracic extracts *in vitro* (see Materials and Methods). p38b deficiency fails to counteract the repressive effect of PCK inhibition on translation. Columns represent means ± the SD ($n = 3$; NS, not significant; *, $P < 0.05$; **, $P < 0.01$ [unpaired two-tailed Student *t* test]). (E) p38b signaling is required for proteotoxic stress-induced dissociation of Rack1 from polysomes. Wild-type and p38b-null animals were treated with puromycin, and thoracic extracts were fractionated by using sucrose gradient centrifugation. Clear redistribution of Rack1 between the RNP (top of gradient) and polysome (bottom of gradient) fractions is observed in puromycin-fed wild-type flies. In *p38b*-null flies Rack1 remains largely associated with the polysomal fraction under proteotoxic stress. (F) Model depicting the mechanisms of Rack1-mediated translational control. A putative ribosome-unbound Rack1 complex that represses translation in response to p38 signaling is shown on the left.

we assessed *de novo* protein synthesis rates in muscles of 1-day-old and 15-day-old flies using an *in vitro* translation assay (Fig. 7A). Thoracic extracts were prepared from adults carrying the *p38b* and *Rack1* alleles, followed by measurement of the translational activity in these extracts using a synthetic firefly luciferase mRNA. Consistent with previous findings (29) in wild-type controls, the translation rates were greatly attenuated in older flies. In contrast, extracts from young homozygous p38b mutants, and to a comparable extent the *Mef2>p38b IR* flies, showed an ~60% higher translation rate, and no significant reduction of translational activity was detected in aged animals. Extracts from young *Rack1*-null muscle displayed a 42% lower translation rate compared to wild-type controls, a finding consistent with a positive regulatory role for Rack1 in protein synthesis. A small further rate reduction was observed in extracts from 15-day-old Rack1 mutants. Importantly, the knockdown of p38b in a Rack1-null background had no effect on the reporter translation rate in extracts from either young or aged flies. These results suggest that the stimulating effect of p38b deficiency on protein translation in thoracic muscle is dependent on Rack1 and place Rack1 downstream of p38b signaling.

Similar results were obtained when we measured protein synthesis rates in thoracic muscle of live flies using SUnSET (30, 31). The incorporation of puromycin into polypeptide chains was visualized by Western blotting of thoracic extracts (Fig. 7B). Wild-type flies show a clear reduction in translation rate upon aging, whereas no appreciable reduction is observed in 15-day-old p38b-deficient flies (*p38bΔ45* and *Mef2>p38b IR*). The effect of p38b deficiency is dependent on Rack1 as protein synthesis rate was found to be low in $Rack1^{1.8}$ flies regardless of the p38b level.

p38b signaling may direct Rack1 to a ribosome-unbound translational repressor complex. Rack1 strongly interacts with the 40S ribosomal subunit and is also present in a 40S-unbound pool. As a component of 40S, Rack1 is generally believed to stimulate translation initiation by recruiting protein kinase C (PKC) to eukaryotic translation initiation factor 6 (eIF6) and eIF4E, but its translational function outside of the 40S complex is poorly understood (26). Therefore, we sought to elucidate the molecular basis of p38b-mediated effect of Rack1 on protein synthesis in muscle. First, we examined the association of Rack1 and individual ribosomal subunits (measured by detecting rpS6 and 28S rRNA) with total mRNA in 1-day-old and 15-day-old wild-type and p38b-null animals. These flies were also carrying a constitutively expressed GFP transgene, providing a model mRNA devoid of regulatory untranslated regions. Oligo(dT) pulldown experiments using tho-

racic extracts from these animals showed a reduced association of 40S and 60S with mRNA in aged wild-type flies compared to younger controls. Consistent with the *in vitro* translation results, in p38b mutants mRNA remained associated with the ribosomal subunits at either age. Importantly, the association of Rack1 with polyadenylated transcripts appears largely unchanged irrespective of age or p38b genotype (Fig. 7C). The dissociation of 40S and 60S subunits but not Rack1 from mRNA in wild-type aged muscle may indicate that p38b signaling induces dissociation of Rack1 from 40S. However, immunoprecipitation of Rack1 from thorax lysates shows that the Rack1-40S complex remains intact in both young and aged muscle and appears independent of p38b. Similarly, GFP mRNA coprecipitates with Rack1 at comparable levels in all samples. In contrast, a clear dissociation of the 60S subunit occurs in aged wild-type muscle, which is consistent with the oligo(dT) pulldown results (Fig. 7C).

Since Rack1 positively regulates translation initiation through PKC, we next tested whether p38b signaling is also involved in this pathway. One-day-old Rack1- and p38b-null flies were treated with a potent inhibitor of PKC, chelerythrine chloride, and the translational activity in muscle extracts was measured in an *in vitro* reaction. Inhibition of PKC potently attenuates translational activity in the wild-type muscle and has no significant effect in Rack1 mutants, confirming the requirement of Rack1 for the translational effects of PKC (Fig. 7D). As seen before (Fig. 7A and B), p38b-null muscle displays elevated translational activity. However, PKC inhibition reduces translation rate proportionally to the change in wild-type muscle, indicating that p38b is dispensable for the Rack1/PKC signaling.

These observations are consistent with the possibility that p38b signaling antagonizes Rack1-dependent potentiation of translational initiation independently of PKC signaling or 80S assembly and promotes the association of Rack1 with mRNA independently of binding to 40S. Furthermore, since p38b deficiency augments basal translation rates, the Rack1-mRNA complex may be translationally repressive (Fig. 7C). To test this model, we subjected wild-type and p38b-null flies to proteotoxic stress and fractionated thoracic extracts on sucrose gradients to separate fractions containing actively translating polysomes from nonribosomal RNP fractions (Fig. 7E). As expected, reduced levels of Rack1 and rpS6 are present in polysomes from stressed wild-type flies. Concomitantly, a significantly higher level of Rack1 is observed in the RNP fraction, in the absence of a corresponding increase in the level of 40S. In p38b mutant animals proteotoxic stress fails to cause a similar redistribution of the ribosomes and Rack1. This result suggests that stress-induced p38b signaling transports Rack1 into a ribosome-unbound pool.

DISCUSSION

Protein homeostasis plays a central role in normal muscle function, aging, and disease. The high level of metabolic activity in muscle tissue creates an environment favoring the accumulation of protein damage. Not surprisingly, the cellular mechanisms controlling protein turnover in this tissue are complex and finely tuned. Pathogenic dysregulation of myoproteostasis causes PAMs, e.g., sIBM, that lead to a progressive decline in muscle function and likely contribute to organismal aging. Since molecular lesions driving sIBM remain elusive, modeling PAMs in genetically tractable organisms may yield much needed insights.

Based on a previous study that documented locomotor deficits in p38b mutant *Drosophila* (17), we examined the accumulation of polyubiquitylated protein aggregates in mutant thoracic muscles and found greatly elevated aggregate levels. Although this result is consistent with a known role of p38 in reducing ROS, and protein oxidative damage, via the Mef2/Sod2 pathway (17), our data suggest additional mechanisms by which p38b antagonizes aggregation. First, constitutive expression of Sod2 displays minimal effect on aggregate levels in either wild-type or p38b deficient muscle. Second, short-term induction of ROS by feeding flies paraquat fails to significantly elevate aggregate levels. In contrast to oxidative damage, puromycin-induced proteotoxic stress potently enhanced aggregate deposition in a p38b-dependent and Sod2-independent manner.

Proteasomal degradation and autophagy mediate clearance of misfolded and damaged proteins, and represent likely downstream effectors of p38b signaling. Indeed, in mammals the Gadd45β/Mekk4/p38 pathway inhibits Atg5 by direct phosphorylation (32), and p38α appears to disrupt cycling-competent Atg9-p38IP complex by competing for p38IP binding (33). Also, the MLK3/p38 pathway induced by the accumulation of mutant GFAP in astrocytes enhances autophagy by negatively regulating phospho-mTOR (34). To determine whether these degradation pathways are the main nodes of the p38b-regulated proteostasis, we used a chemical genetic approach. Strikingly, pharmacologic inhibition of proteasome, autophagy, or both failed to rescue aggregation-promoting effect of p38b deficiency, arguing for the existence of p38b-regulated processes upstream of the degradation pathways.

Previously, it has been shown that p38 activates its substrate kinases Mnk1/Mnk2 that bind to eIF4G and phosphorylate the Ser201 residue of eIF4E (35), thereby potentiating translation initiation. Among the 19 putative p38b substrates isolated in our *in vivo* proteomic screen two, rpS15 and Rack1, are ribosomal components potentially providing a direct link between p38 signaling and translational activity. Rack1 is a highly conserved multifunctional WD-repeat adaptor protein that binds 40S through 18S rRNA, rpS3, rpS16, and rpS17 (26). Our biochemical analyses confirmed that p38b specifically phosphorylates Rack1 on Ser and Thr residues, although specific phosphorylation sites remain to be determined. Importantly, p38b-Rack1 signaling appears unidirectional, since no Rack1-dependent change in p38b activity is observed. Genetic evidence further supports our hypothesis that p38b and Rack1 operate in a common pathway influencing aggregate formation in muscle. Thus, a Rack1 hypomorphic mutation that by itself is insufficient to cause high level of aggregates, synergizes with the RNAi-mediated depletion of p38b to cause significantly augmented aggregate deposition, locomotor defects, and shortened life-span.

What is the molecular mechanism of the p38b/Rack1-mediated control of myoproteostasis? Previous studies highlighted both stimulatory and inhibitory roles of Rack1 in mRNA translation depending on cellular context. As a positive regulator of translation initiation, Rack1 recruits activated PKCβII to the ribosome to phosphorylate eIF6 (36) and eIF4E (37). However, Rack1 associates with the ribosome even in cell types that lack PKCβII expression, suggesting additional roles for the ribosome-bound Rack1. Other studies note elevated translational activity in Rack1-deficient cells (38, 39). Extracts from thoracic muscle of Rack1-null mutants display a reduced activity in *in vitro* translation assays compared to wild-type controls, whereas p38b mutant

extracts show elevated activity. However, the effect of p38b depletion is fully reversed in the Rack1-null background, implicating p38b as a negative upstream regulator of a Rack1-dependent translation pathway. Pharmacologic inhibition of PKC represses translational activity in p38b-null thoracic extracts, suggesting that p38b/Rack1 signaling is independent of the PKC pathway and raising the possibility that p38b acts on Rack1 outside of the Rack1-PKC-80S complex (Fig. 7F). Biochemical fractionation experiments lend support to this model. First, in wild-type aged muscle, reduced translational activity coincides with an attenuated association of mRNA with the 40S and 60S subunits but not Rack1 (Fig. 7C). Second, proteotoxic stress causes an increase of Rack1 level in a nonpolysomal fraction without the corresponding increase in 40S (Fig. 7E). Both of these effects exhibit p38b dependence.

The molecular identity of stress-induced and potentially ribosome-unbound Rack1 complex and its effect on the translation of associated mRNA in *Drosophila* are unknown. A recent study in yeast (40) characterized a Rack1-containing translationally repressive SESA complex that may be conserved in higher eukaryotes. The SESA complex comprises the KH-domain RNA-binding protein Scp160/vigilin, an eIF4E-binding protein Eap1, Smy2/GIGYF2, and Asc1/Rack1 and becomes activated by the spindle pole body duplication defects to repress the translation of a subset of cellular mRNAs, e.g., *POM34* mRNA. Our interaction proteomics experiments identified a homologous Rack1/vigilin/GIGYF2 repressive complex in human cells that displays responsiveness to stressful stimuli (V. Belozerov, unpublished data), offering a candidate mechanistic link between p38 signaling and translational repression.

ACKNOWLEDGMENTS

This study was funded by the Canadian Institutes of Health Research and Natural Sciences and Engineering Research Council of Canada grants to J.C.M.

We are grateful to Anne-Claude Gingras for help with proteomic experiments and short-term salary support for V.E.B. We thank the Bloomington *Drosophila* Stock Center for fly stocks and Alysia Vrailas-Mortimer and Subhabrata Sanyal (Emory University) for p38b mutant flies and DNA constructs.

REFERENCES

1. **Nair KS.** 2005. Aging muscle. Am. J. Clin. Nutr. **81:**953–963.
2. **Rera M, Azizi MJ, Walker DW.** 2013. Organ-specific mediation of lifespan extension: more than a gut feeling? Ageing Res. Rev. **12:**436–444. http://dx.doi.org/10.1016/j.arr.2012.05.003.
3. **Demontis F, Perrimon N.** 2010. FOXO/4E-BP signaling in *Drosophila* muscles regulates organism-wide proteostasis during aging. Cell **143:**813–825. http://dx.doi.org/10.1016/j.cell.2010.10.007.
4. **Balch WE, Morimoto RI, Dillin A, Kelly JW.** 2008. Adapting proteostasis for disease intervention. Science **319:**916–919. http://dx.doi.org/10.1126/science.1141448.
5. **Robertson AL, Bottomley SP.** 2010. Towards the treatment of polyglutamine diseases: the modulatory role of protein context. Curr. Med. Chem. **17:**3058–3068. http://dx.doi.org/10.2174/092986710791959800.
6. **Askanas V, Engel WK.** 2008. Inclusion-body myositis: muscle-fiber molecular pathology and possible pathogenic significance of its similarity to Alzheimer's and Parkinson's disease brains. Acta Neuropathol. **116:**583–595. http://dx.doi.org/10.1007/s00401-008-0449-0.
7. **Schröder R.** 2013. Protein aggregate myopathies: the many faces of an expanding disease group. Acta Neuropathol. **125:**1–2. http://dx.doi.org/10.1007/s00401-012-1071-8.
8. **Askanas V, Engel WK, Nogalska A.** 2009. Inclusion body myositis: a degenerative muscle disease associated with intra-muscle fiber multi-protein aggregates, proteasome inhibition, endoplasmic reticulum stress and decreased lysosomal degradation. Brain Pathol. **19:**493–506. http://dx.doi.org/10.1111/j.1750-3639.2009.00290.x.
9. **Machado P, Miller A, Holton J, Hanna M.** 2009. Sporadic inclusion body myositis: an unsolved mystery. Acta Rheumatol. Port. **34:**161–182.
10. **Luheshi LM, Crowther DC, Dobson CM.** 2008. Protein misfolding and disease: from the test tube to the organism. Curr. Opin. Chem. Biol. **12:**25–31. http://dx.doi.org/10.1016/j.cbpa.2008.02.011.
11. **Jones MA, Grotewiel M.** 2011. *Drosophila* as a model for age-related impairment in locomotor and other behaviors. Exp. Gerontol. **46:**320–325. http://dx.doi.org/10.1016/j.exger.2010.08.012.
12. **Kim C, Srivastava S, Rice M, Godenschwege TA, Bentley B, Ravi S, Shao S, Woodard CT, Schwartz LM.** 2011. Expression of human amyloid precursor protein in the skeletal muscles of *Drosophila* results in age- and activity-dependent muscle weakness. BMC Physiol. **11:**7. http://dx.doi.org/10.1186/1472-6793-11-7.
13. **Chartier A, Benoit B, Simonelig M.** 2006. A *Drosophila* model of oculopharyngeal muscular dystrophy reveals intrinsic toxicity of PABPN1. EMBO J. **25:**2253–2262. http://dx.doi.org/10.1038/sj.emboj.7601117.
14. **Wang Y, Melkani GC, Suggs JA, Melkani A, Kronert WA, Cammarato A, Bernstein SI.** 2012. Expression of the inclusion body myopathy 3 mutation in *Drosophila* depresses myosin function and stability and recapitulates muscle inclusions and weakness. Mol. Biol. Cell **23:**2057–2065. http://dx.doi.org/10.1091/mbc.E12-02-0120.
15. **Lluís F, Perdiguero E, Nebreda AR, Muñoz-Cánoves P.** 2006. Regulation of skeletal muscle gene expression by p38 MAP kinases. Trends Cell Biol. **16:**36–44. http://dx.doi.org/10.1016/j.tcb.2005.11.002.
16. **Perdiguero E, Ruiz-Bonilla V, Serrano AL, Muñoz-Cánoves P.** 2007. Genetic deficiency of p38α reveals its critical role in myoblast cell cycle exit: the p38α-JNK connection. Cell Cycle **6:**1298–1303. http://dx.doi.org/10.4161/cc.6.11.4315.
17. **Vrailas-Mortimer A, del Rivero T, Mukherjee S, Nag S, Gaitanidis A, Kadas D, Consoulas C, Duttaroy A, Sanyal S.** 2011. A muscle-specific p38 MAPK/Mef2/MnSOD pathway regulates stress, motor function, and life span in *Drosophila*. Dev. Cell **21:**783–795. http://dx.doi.org/10.1016/j.devcel.2011.09.002.
18. **Griciuc A, Aron L, Roux MJ, Klein R, Giangrande A, Ueffing M.** 2010. Inactivation of VCP/ter94 suppresses retinal pathology caused by misfolded rhodopsin in *Drosophila*. PLoS Genet. **6:**e1001075. http://dx.doi.org/10.1371/journal.pgen.1001075.
19. **Belozerov VE, Lin ZY, Gingras AC, McDermott JC, Michael Siu KW.** 2012. High-resolution protein interaction map of the *Drosophila melanogaster* p38 mitogen-activated protein kinases reveals limited functional redundancy. Mol. Cell. Biol. **32:**3695–3706. http://dx.doi.org/10.1128/MCB.00232-12.
20. **Liu G, Zhang J, Larsen B, Stark C, Breitkreutz A, Lin ZY, Breitkreutz BJ, Ding Y, Colwill K, Pasculescu A, Pawson T, Wrana JL, Nesvizhskii AI, Raught B, Tyers M, Gingras AC.** 2010. ProHits: integrated software for mass spectrometry-based interaction proteomics. Nat. Biotechnol. **28:**1015–1017. http://dx.doi.org/10.1038/nbt1010-1015.
21. **Gebauer F, Hentze MW.** 2007. Studying translational control in *Drosophila* cell-free systems. Methods Enzymol. **429:**23–33. http://dx.doi.org/10.1016/S0076-6879(07)29002-0.
22. **Rakotondrafara AM, Hentze MW.** 2011. An efficient factor-depleted mammalian in vitro translation system. Nat. Protoc. **6:**563–571. http://dx.doi.org/10.1038/nprot.2011.314.
23. **Qin X, Ahn S, Speed TP, Rubin GM.** 2007. Global analyses of mRNA translational control during early *Drosophila* embryogenesis. Genome Biol. **8:**R63. http://dx.doi.org/10.1186/gb-2007-8-4-r63.
24. **Ota A, Zhang J, Ping P, Han J, Wang Y.** 2010. Specific regulation of noncanonical p38α activation by Hsp90-Cdc37 chaperone complex in cardiomyocyte. Circ. Res. **106:**1404–1412. http://dx.doi.org/10.1161/CIRCRESAHA.109.213769.
25. **Han J, Jiang Y, Li Z, Kravchenko VV, Ulevitch RJ.** 1997. Activation of the transcription factor MEF2C by the MAP kinase p38 in inflammation. Nature **386:**296–299. http://dx.doi.org/10.1038/386296a0.
26. **Adams DR, Ron D, Kiely PA.** 2011. RACK1, A multifaceted scaffolding protein: structure and function. Cell Commun. Signal. **9:**22. http://dx.doi.org/10.1186/1478-811X-9-22.
27. **Dhanasekaran DN, Kashef K, Lee CM, Xu H, Reddy EP.** 2007. Scaffold proteins of MAP-kinase modules. Oncogene **26:**3185–3202. http://dx.doi.org/10.1038/sj.onc.1210411.
28. **Kadrmas JL, Smith MA, Pronovost SM, Beckerle MC.** 2007. Character-

ization of RACK1 function in *Drosophila* development. Dev. Dyn. **236:** 2207–2215. http://dx.doi.org/10.1002/dvdy.21217.

29. **Webster GC, Beachell VT, Webster SL.** 1980. Differential decrease in protein synthesis by microsomes from aging *Drosophila melanogaster*. Exp. Gerontol. **15:**495–497. http://dx.doi.org/10.1016/0531-5565(80)90058-3.
30. **Schmidt EK, Clavarino G, Ceppi M, Pierre P.** 2009. SUnSET, a nonradioactive method to monitor protein synthesis. Nat. Methods **6:**275–277. http://dx.doi.org/10.1038/nmeth.1314.
31. **Goodman CA, Mabrey DM, Frey JW, Miu MH, Schmidt EK, Pierre P, Hornberger TA.** 2011. Novel insights into the regulation of skeletal muscle protein synthesis as revealed by a new nonradioactive in vivo technique. FASEB J. **25:**1028–1039. http://dx.doi.org/10.1096/fj.10-168799.
32. **Keil E, Höcker R, Schuster M, Essmann F, Ueffing N, Hoffman B, Liebermann DA, Pfeffer K, Schulze-Osthoff K, Schmitz I.** 2013. Phosphorylation of Atg5 by the Gadd45β-MEKK4-p38 pathway inhibits autophagy. Cell Death Differ. **20:**321–332. http://dx.doi.org/10.1038/cdd.2012.129.
33. **Webber JL, Tooze SA.** 2010. Coordinated regulation of autophagy by p38α MAPK through mAtg9 and p38IP. EMBO J. **29:**27–40. http://dx.doi.org/10.1038/emboj.2009.321.
34. **Tang G, Yue Z, Talloczy Z, Hagemann T, Cho W, Messing A, Sulzer DL, Goldman JE.** 2008. Autophagy induced by Alexander disease-mutant GFAP accumulation is regulated by p38/MAPK and mTOR signaling pathways. Hum. Mol. Genet. **17:**1540–1555. http://dx.doi.org/10.1093/hmg/ddn042.
35. **Shveygert M, Kaiser C, Bradrick SS, Gromeier M.** 2010. Regulation of eukaryotic initiation factor 4E (eIF4E) phosphorylation by mitogen-activated protein kinase occurs through modulation of Mnk1-eIF4G interaction. Mol. Cell. Biol. **30:**5160–5167. http://dx.doi.org/10.1128/MCB.00448-10.
36. **Ceci M, Gaviraghi C, Gorrini C, Sala LA, Offenhäuser N, Marchisio PC, Biffo S.** 2003. Release of eIF6 (p27BBP) from the 60S subunit allows 80S ribosome assembly. Nature **426:**579–584. http://dx.doi.org/10.1038/nature02160.
37. **Ruan Y, Sun L, Hao Y, Wang L, Xu J, Zhang W, Xie J, Guo L, Zhou L, Yun X, Zhu H, Shen A, Gu J.** 2012. Ribosomal RACK1 promotes chemoresistance and growth in human hepatocellular carcinoma. J. Clin. Invest. **122:**2554–2566. http://dx.doi.org/10.1172/JCI58488.
38. **Gerbasi VR, Weaver CM, Hill S, Friedman DB, Link AJ.** 2004. Yeast Asc1p and mammalian RACK1 are functionally orthologous core 40S ribosomal proteins that repress gene expression. Mol. Cell. Biol. **24:**8276–8287. http://dx.doi.org/10.1128/MCB.24.18.8276-8287.2004.
39. **Kuroha K, Akamatsu M, Dimitrova L, Ito T, Kato Y, Shirahige K, Inada T.** 2010. Receptor for activated C kinase 1 stimulates nascent polypeptide-dependent translation arrest. EMBO Rep. **11:**956–961. http://dx.doi.org/10.1038/embor.2010.169.
40. **Sezen B, Seedorf M, Schiebel E.** 2009. The SESA network links duplication of the yeast centrosome with the protein translation machinery. Genes Dev. **23:**1559–1570. http://dx.doi.org/10.1101/gad.524209.